

P4.13

A NUMERICAL STUDY OF THE EFFECTS OF LARGE EDDIES ON  
PHOTOCHEMISTRY IN THE CONVECTIVE BOUNDARY LAYER

Jerold A. Herwehe\*

NOAA/ARL/Atmospheric Turbulence & Diffusion Division, Oak Ridge, Tennessee

Richard T. McNider and Michael J. Newchurch

University of Alabama in Huntsville, Huntsville, Alabama

1. INTRODUCTION

Under clear sky conditions, daytime solar heating of the ground surface causes thermal instability and the formation of buoyant parcels of air, which combine to produce organized structures ranging in scale from the convective boundary layer (CBL) depth (1-2 km) down to the Kolmogorov microscale (~1 mm). When considering photochemistry, the vast majority of trace gas emissions take place near the earth's surface, usually within the CBL. During the daytime, these emissions are caught up in the turbulent eddies of the CBL. The turbulent nature of the CBL would normally imply that all trace gases and other scalar quantities are well-mixed. Reactive surface-emitted gases might be expected to decrease monotonically in mixing ratio with height. However, observational data have shown significant concentration variations within the CBL for some trace species. Andronache *et al.* (1994) presented several complex profiles of isoprene, a gas emitted from surface vegetation, gathered during a Southern Oxidants Study (SOS) field experiment. These isoprene profiles showed unexpected mixing ratio maxima at heights well above the surface.

The observed structure in many trace gas profiles is a result of the nonlinear interaction of the turbulence and the photochemical transformation processes. The chemical lifetimes of important trace gases can range from fractions of a second (e.g., OH) to years (e.g., CH<sub>4</sub>). Convective overturning of large eddies within the CBL occurs on a time scale of 10-20 minutes. Shorter-lived trace gases react on time scales on the order of the convective time scale, or faster, leading to concentration fluctuations for these species. Sykes *et al.* (1994) emphasized that if the reaction rate between two reactants is relatively fast compared to the turbulent mixing rate, then the reactants cannot be brought together quickly enough by the turbulent cascade process and, hence, the overall reaction rate will be controlled by the turbulence time scales. The effect of the turbulence on the fast reactions operates on the trace gas prognostic equations via a concentration fluctuation covariance term (of the form  $\overline{A'B'}$ ) which is neglected in most photochemical models.

The purpose of this study was to develop a high temporal and spatial resolution 3-D coupled dynamical and photochemical numerical model that properly

accounts for concentration fluctuations and turbulent mixing effects on reactivity. The new model was tested with two idealized photochemical scenarios.

2. COUPLED MODELING APPROACH

Previous studies (e.g., Sykes *et al.*, 1994), investigated the effects of turbulence on a single irreversible reaction using large-eddy simulation (LES), a technique where large, energy-containing eddies are resolved explicitly in a 3-D, time-dependent numerical simulation of the CBL. In LES, only small, subgrid-scale motions are parameterized. Moeng (1998) provides an overview of LES modeling. To make the new coupled model useful beyond the usual idealized situations simulated by specialized LES codes, the Regional Atmospheric Modeling System (RAMS) mesoscale model (Pielke *et al.*, 1992) was chosen as the model component to generate the LES dynamics.

The second component of the new coupled model solves the trace gas photochemical reactions. Due to the wide disparity in the chemical time scales of the individual species involved in most atmospheric chemistry problems, the resulting system of ordinary differential equations (ODEs) forms a "stiff" system of equations. Solving the stiff ODEs of chemical kinetics problems limits the maximum allowable time step size to the smallest characteristic time scales of the most reactive species in order to maintain computational stability. A Gear-type solver is the standard method used to accurately solve a stiff ODE system. A highly accurate chemistry solver was deemed essential for the new coupled model, so the second-generation Sparse Matrix Vectorized Gear (SMVGEAR II) solver was chosen (Jacobson, 1995 and 1998).

The SMVGEAR II chemistry solver was integrated into the RAMS model to form the coupled Large-Eddy Simulation with chemistry (LESchem) model. Construction of LESchem preserved all of the original features and capabilities found in RAMS and SMVGEAR II. The coupling of the dynamics and photochemistry occurs during each fixed LES dynamics time step as follows: 1) RAMS supplies SMVGEAR II with current 3-D temperature, pressure, and trace gas distributions; 2) SMVGEAR II uses these values to solve the photochemical reactions over the duration of the dynamics time step using variable time step sizes, then passes back the updated trace gas fields; and 3) RAMS then emits, (dry) deposits, transports, and diffuses these trace gases throughout the domain while also computing the LES dynamics. Steps 1-3 repeat for

\* Corresponding author address: Jerold A. Herwehe, NOAA/ATDD, 456 S. Illinois Ave., P.O. Box 2456, Oak Ridge, TN 37831-2456; e-mail: herwehe@atdd.noaa.gov.

each dynamics time step. Thus, the LESchem model computes the LES dynamics and chemical transformations each time step in a directly coupled fashion. This design also allows for future bidirectional feedbacks between the dynamics and the chemistry.

### 3. COUPLED LES-PHOTOCHEMISTRY RESULTS

To test the LESchem model, two idealized midday photochemical scenarios were simulated based on the 4 August 1991 meteorological and trace gas observational data available from the Giles County, TN, SOS site (35.18° N latitude, 87.2° W longitude). A simplified gas-phase isoprene photochemical mechanism from Biazar (1995) (based upon Trainer *et al.*, 1987; Trainer *et al.*, 1991) was used. This condensed isoprene mechanism consists of 45 trace gas species undergoing nonlinear chemical transformations via 77 kinetic and 15 photolytic reactions (see Herwehe, 2000, for details). Both scenarios started from the same set of trace gas initial profiles (except for NO) and both scenarios specified dry deposition velocities at the surface for 15 trace species, such as O<sub>3</sub>, HNO<sub>3</sub>, NO<sub>2</sub>, and some organic compounds, for example. All coupled simulations reported here were computed in 64-bit precision on a personal computer (PC).

#### 3.1 Simulated Convective Boundary Layer

Identical LES CBL dynamics were generated during the simulation of each photochemical scenario. The idealized LES in this study simulates a dry turbulent midday CBL under clear sky with horizontally homogeneous surface and initial conditions, with no mean wind. Based on midday potential temperature profile data appropriate for the Giles County site, the CBL depth  $z_i$  was expected to be around 2 km. Since the horizontal scale of buoyancy driven updrafts is typically  $1.5z_i$ , the domain was chosen to be on the order of 10 km per side to capture the large eddy characteristics of several convective plumes. In contrast to many LESs which define the CBL height to coincide with the domain top at 1-2 km, the LESchem domain height for this study was chosen to be 4 km to adequately separate the top boundary condition and its effects from the top of the CBL. The domain was discretized to 50  $x$  by 50  $y$  by 41  $z$  grid points with a uniform horizontal grid resolution of 200 m and a vertical grid resolution of 100 m. Nested grids were not used for the LES. The bottom of the domain is flat and homogeneous. A rigid lid was specified at the top boundary by forcing the vertical velocity to be zero there. In order to damp out gravity waves and prevent other disturbances from reflecting off the top boundary, a Rayleigh friction absorbing layer was specified in the stable air of the top six grid levels with a maximum dissipation time scale of 200 s at the top, linearly decreasing to zero by the fifth level below the domain top. Lateral boundary conditions were periodic.

To produce the LES, the RAMS component of LESchem was run in nonhydrostatic mode using a hybrid (leapfrog and forward) time differencing scheme

with a time step size of 3 s. The simulated time was 2 hr starting at local noon. The radiation and soil models were disabled, so the convection was driven by a constant surface heating of about 230 W m<sup>-2</sup>. A roughness length of 0.40 m was specified to represent a fairly dense forest on level terrain. The cloud microphysics model and surface moisture flux were also disabled, so the LES is a dry atmosphere not influenced by water vapor sources, sinks, or phase changes. Diffusion in the LES was parameterized by the Deardorff scheme through the use of a prognostic subgrid turbulent kinetic energy (TKE) equation. A random initial near-surface potential temperature perturbation within the range of  $\pm 1.0$  K was utilized to help initiate the convection in the calm initial conditions.

Figure 1 shows sample slices of the instantaneous wind vectors taken from the end of the 2-hr LES. The computed horizontally-averaged CBL depth is 2100 m with a convective velocity scale  $w_*$  of 2.2 m s<sup>-1</sup>, which yields a convective time scale  $t_*$  of 15.6 min. The

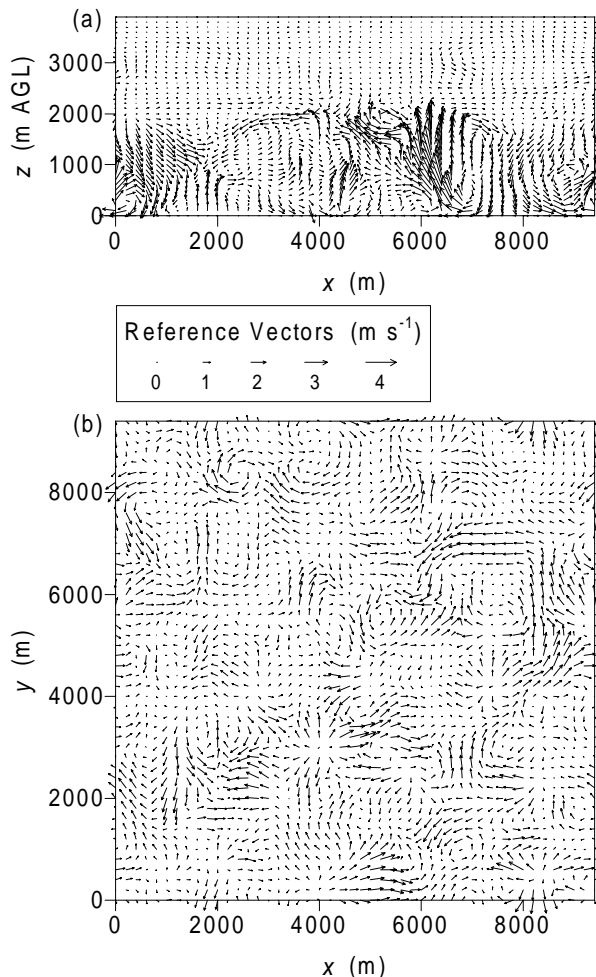


Figure 1. Final LES wind vectors from (a) a vertical slice located at  $y = 5800$  m and (b) a horizontal slice located near mid-CBL at  $z = 1000$  m. Scale reference vectors are shown between the two plot frames.

vertical slice of Figure 1a shows turbulent eddies of various sizes, with one large sweeping updraft of about  $4 \text{ m s}^{-1}$  over  $x = 6200 \text{ m}$ . The horizontal mid-CBL slice of Figure 1b exhibits the secondary circulations and vorticity induced by the convective plumes and thermals. Updrafts occupy 39% of the horizontal area at mid-CBL, and about 38% of the area at  $z = 1900 \text{ m}$ . However, near the surface at  $z = 100 \text{ m}$ , the buoyant updrafts account for only 48% of the horizontal area and have not yet formed large convective plumes, but instead form connected filamentary convective sheets or cell walls surrounding weaker downdrafts.

Figure 2 shows the horizontally-averaged normalized wind component variance and the normalized kinematic heat flux profiles taken from the end of the LES. The computed convective temperature scale  $\theta_*$  is  $0.08 \text{ K}$  with a surface kinematic heat flux of about  $0.19 \text{ K m s}^{-1}$ . Resolvable TKE had a maximum value of around  $1.25 \text{ m}^2 \text{ s}^{-2}$  at  $1/3 z_i$ . Comparison of these and additional turbulence statistics to those from other studies confirmed that the present LES gives a realistic representation of a dry midday turbulent CBL.

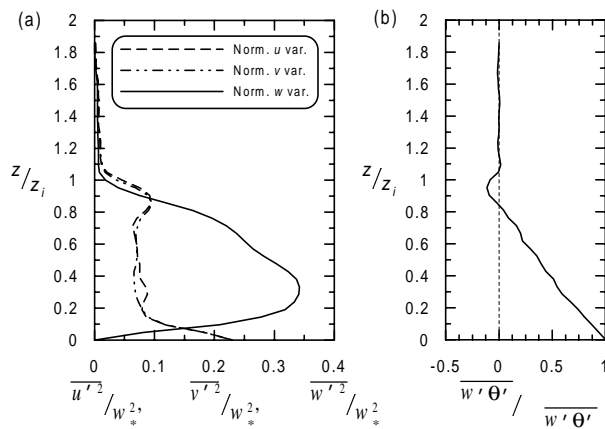


Figure 2. Sample horizontally-averaged LES CBL statistics: (a) normalized wind component variances and (b) normalized heat flux.

### 3.2 CASE1: Isoprene and NO Coemitting

The first idealized scenario, CASE1, specified isoprene (ISOP) and NO to be coemitting continuously and uniformly from the bottom surface to represent homogeneously mixed vegetation with active soil microbe emissions. Figure 3 shows a vertical slice of ISOP from the same location as Figure 1a at the end of the coupled simulation. Note the higher ISOP mixing ratios being drawn up from the surface into the convective plumes. Also note the pockets of relatively high ISOP mixing ratios present high in the CBL, while relatively low ISOP amounts can be seen in downdraft parcels located low in the CBL. This illustrates that, due to its chemical lifetime, isoprene is not well mixed in the CBL even in the presence of turbulent eddies. Longer-lived trace gases, such as  $\text{O}_3$ , are well mixed, showing very little structure in their CBL distribution.

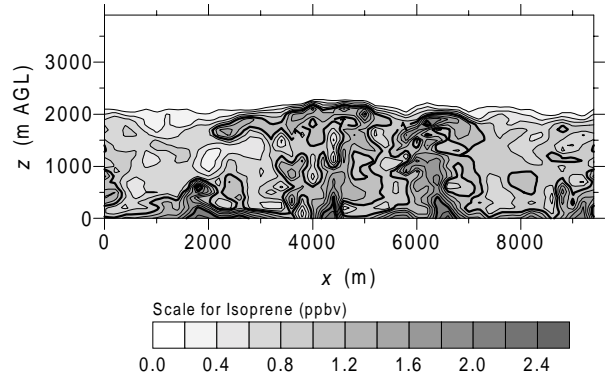


Figure 3. CASE1 LES final ISOP mixing ratio from a vertical slice located at  $y = 5800 \text{ m}$ .

To emulate a typical air quality model for comparison purposes, the LESchem model was reconfigured to perform a coupled first-order ( $K$ -theory) closure mesoscale simulation of the CASE1 photochemical scenario. The  $100 \text{ m}$  vertical grid resolution was retained, but the horizontal grid spacing was multiplied by a factor of 20 so that  $\Delta x = \Delta y = 4 \text{ km}$ , and hydrostatic balance was specified. Of course, the mesoscale dynamics display no eddy motions in the boundary layer. Sample final time horizontally-averaged LES- and mesoscale-run trace gas profiles are shown in Figure 4. Volume-averaged mixing ratio comparisons revealed that at the end of the simulations, there was little difference in total amounts of ISOP between the LES and mesoscale runs (though their vertical distributions were markedly different), but the LES run had nearly 14% less  $\text{NO}_2$  and around 20% less nitrous acid (HONO) than the mesoscale version of CASE1. The differences in LES and mesoscale trace gas amounts generally occur near the top of the CBL in the entrainment zone. This is due to the vigorous reactant-laden thermals of the LES punching into the inversion base and causing additional mixing of available reactants from above the CBL, unlike the mesoscale run which has negligible eddy diffusivity values at the CBL top which prevent much mixing of reactants there.

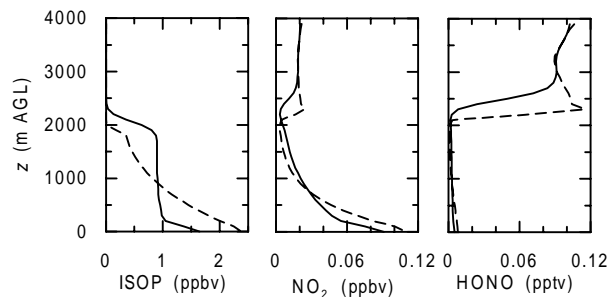


Figure 4. Comparison of the CASE1 mesoscale (dashed) and LES (solid) horizontally-averaged mixing ratio profiles for selected trace gases.

### 3.3 CASE2: Isoprene Emitting into NO-Rich CBL

The second idealized scenario, CASE2, specified that isoprene alone would be continuously emitting from the surface into an initially high background mixing ratio (4 ppbv) of NO in order to represent a fresh urban plume that has rapidly advected over an adjacent forested area. The purpose of CASE2 was to introduce more segregation in the primary effluents, and to provide more NO<sub>x</sub> (=NO+NO<sub>2</sub>) to the otherwise NO<sub>x</sub>-limited regime of CASE1. There was no net production of O<sub>3</sub> during the 2-hr CASE1 simulation, but the enhanced initial NO of CASE2 produced a 17 ppbv (46%) increase in O<sub>3</sub> in the CBL by simulation end.

A mesoscale version of CASE2 was also produced. Final horizontally-averaged mixing ratio profiles for ISOH, NO<sub>2</sub>, and HONO are shown in Figure 5. ISOH is the product of the reaction of ISOP and OH. Comparison of the volume-averaged mixing ratios for these gases showed almost no difference between the LES and mesoscale amounts for NO<sub>2</sub>. The CASE2 LES run ended with over 8% less HONO, but greater than 45% more ISOH than the mesoscale run. As in CASE1, these differences are generally due to the more active LES dynamics present near the top of the CBL.

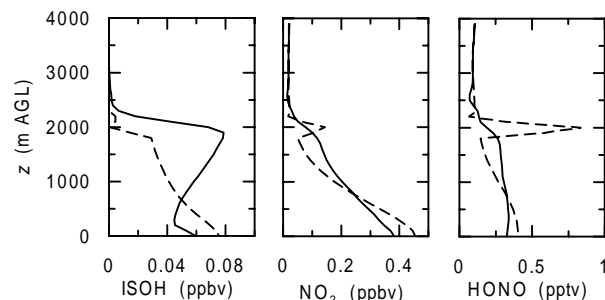


Figure 5. Comparison of the CASE2 mesoscale (dashed) and LES (solid) horizontally-averaged mixing ratio profiles for selected trace gases.

## 4. CONCLUSIONS

The new coupled large-eddy simulation with chemistry (LESchem) model can be used to assess the impact of modeling photochemistry with chemical reactions based on mean concentrations versus reactions based on explicitly simulated instantaneous local trace species concentrations. For the idealized 2-hr coupled simulations conducted here, it was found that first-order closure performs reasonably well at modeling the large scale photochemistry of the midday convective boundary layer. However, the LES to mesoscale differences in trace gas amounts found in the boundary layer entrainment zone could become significant over longer time integration due to the cumulative differences in trace gas exchange between the CBL and the free troposphere of the two modeling techniques. Though not too important in the homogeneous idealized cases of this study, the segregation of some reactants is expected to become more significant when modeling patchy or otherwise

heterogeneous surface emissions and characteristics. A full description of this coupled LES-photochemistry numerical study can be found in Herwehe (2000).

**Acknowledgments:** This research was mainly supported by the NOAA/Air Resources Laboratory's Atmospheric Turbulence and Diffusion Division and by NOAA's *Health of the Atmosphere Program*. Additional support was provided through cooperative agreements with the University of Alabama in Huntsville and North Carolina State University as part of SOS.

## REFERENCES

- Andronache, C., W. L. Chameides, M. O. Rodgers, J. Martinez, P. Zimmerman, and J. Greenberg, 1994: Vertical distribution of isoprene in the lower boundary layer of the rural and urban southern United States. *J. Geophys. Res.*, **99**, 16,989-16,999.
- Biazar, A. P., 1995: The role of natural nitrogen oxides in ozone production in the Southeastern environment. Ph. D. dissertation, Atmospheric Science Program, University of Alabama in Huntsville.
- Herwehe, J. A., 2000: A numerical study of the effects of large eddies on trace gas measurements and photochemistry in the convective boundary layer. Ph. D. dissertation, Department of Atmospheric Science, University of Alabama in Huntsville.
- Jacobson, M. Z., 1995: Computation of global photochemistry with SMVGEAR II. *Atmos. Environ.*, **29**, 2541-2546.
- Jacobson, M. Z., 1998: Improvement of SMVGEAR II on vector and scalar machines through absolute error tolerance control. *Atmos. Environ.*, **32**, 791-796.
- Moeng, C.-H., 1998: Large eddy simulation of atmospheric boundary layers. In *Clear and Cloudy Boundary Layers*, edited by A. A. M. Holtslag and P. G. Duynkerke, pp. 67-84, Royal Netherlands Academy of Arts and Sciences, Amsterdam, The Netherlands.
- Pielke, R. A., W. R. Cotton, R. L. Walko, C. J. Tremback, W. A. Lyons, L. D. Grasso, M. E. Nicholls, M. D. Moran, D. A. Wesley, T. J. Lee, and J. H. Copeland, 1992: A comprehensive meteorological modeling system - RAMS. *Meteorol. Atmos. Phys.*, **49**, 69-91.
- Sykes, R. I., S. F. Parker, D. S. Henn, and W. S. Lewellen, 1994: Turbulent mixing with chemical reaction in the planetary boundary layer. *J. Appl. Meteorol.*, **33**, 825-834.
- Trainer, M., E. Y. Hsie, S. A. McKeen, R. Tallamraju, D. D. Parrish, F. C. Fehsenfeld, and S. C. Liu, 1987: Impact of natural hydrocarbons on hydroxyl and peroxy radicals at a remote site. *J. Geophys. Res.*, **92**, 11,879-11,894.
- Trainer, M., M. P. Buhr, C. M. Curran, F. C. Fehsenfeld, E. Y. Hsie, S. C. Liu, R. B. Norton, D. D. Parrish, E. J. Williams, B. W. Gandrud, B. A. Ridley, J. D. Shetter, E. J. Allwine, and H. H. Westberg, 1991: Observations and modeling of the reactive nitrogen photochemistry at a rural site. *J. Geophys. Res.*, **96**, 3045-3063.